

Supporting Information

Novel Dual-function SERS Identification Strategy for Preliminary Screening and Accurate Diagnosis of Circulating Tumor Cells

Dinghu Zhang^{1,2,3,†}, Jie Lin^{2,3*,†}, Yanping Xu^{1,2,3}, Xiaoxia Wu^{1,2,3}, Xiawei Xu^{2,3}, Yujiao Xie^{2,3}, Ting Pan¹, Yiwei He¹, Jun Luo¹, Zhewei Zhang¹, LinYin Fan¹, Shunxiang Li^{2,3}, Tianxiang Chen^{2,3}, Aiguo Wu^{2,3*} & Guoliang Shao^{1*}

1 Department of Interventional Radiology, Zhejiang Cancer Hospital, Hangzhou Institute of Medicine (HIM), Chinese Academy of Sciences, Hangzhou, Zhejiang 310022, China

2 Ningbo Cixi Institute of Biomedical Engineering, International Cooperation Base of Biomedical Materials Technology and Application, Chinese Academy of Science (CAS) Key Laboratory of Magnetic Materials and Devices and Zhejiang Engineering Research Center for Biomedical Materials, Ningbo Institute of Materials Technology and Engineering, CAS, Ningbo 315201, P.R. China.

3 Advanced Energy Science and Technology Guangdong Laboratory, Huizhou 516000, P.R. China.

† D. H. Zhang and J. Lin contributed equally to this work.

*Corresponding author: (E-mail: linjie@nimte.ac.cn, aiguo@nimte.ac.cn, shaogl@zjcc.org.cn)

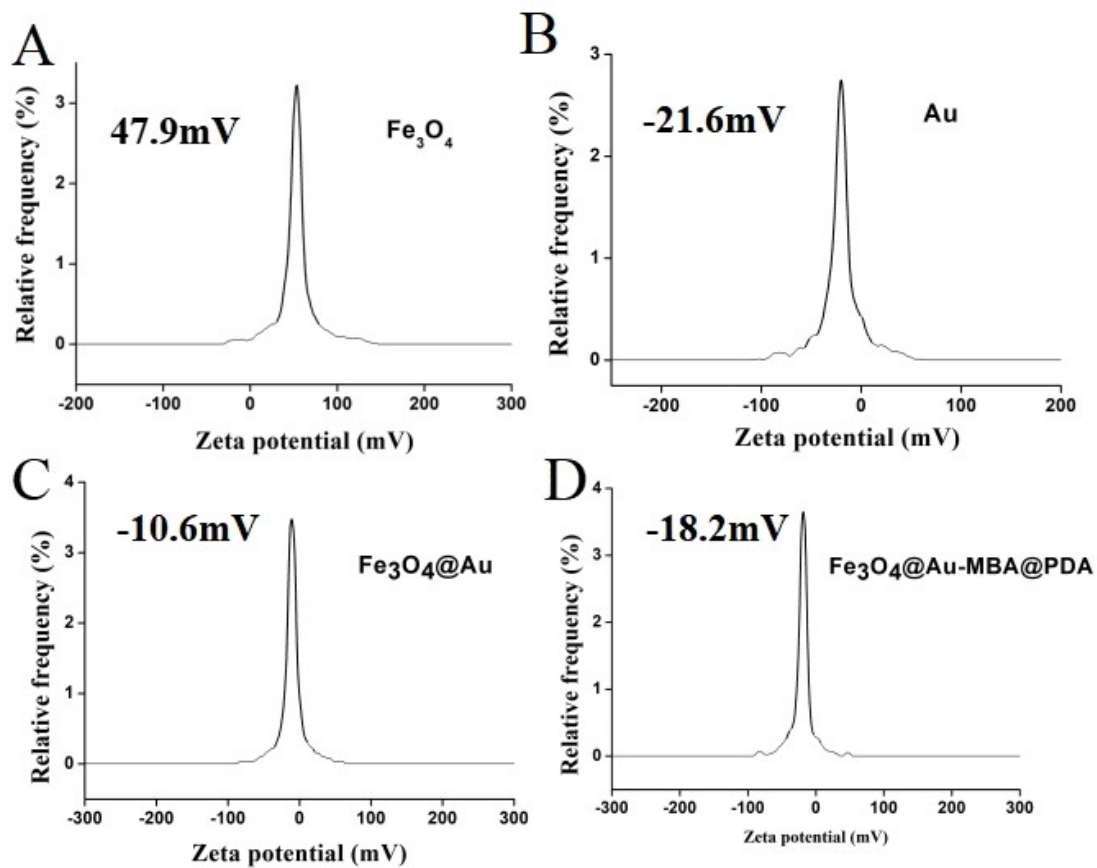


Figure S1. Zeta potential of Fe_3O_4 NPs (A), Au NPs (B), $\text{Fe}_3\text{O}_4@Au$ NPs (C) and $\text{Fe}_3\text{O}_4@Au\text{-MBA@PDA}$ (D), respectively.

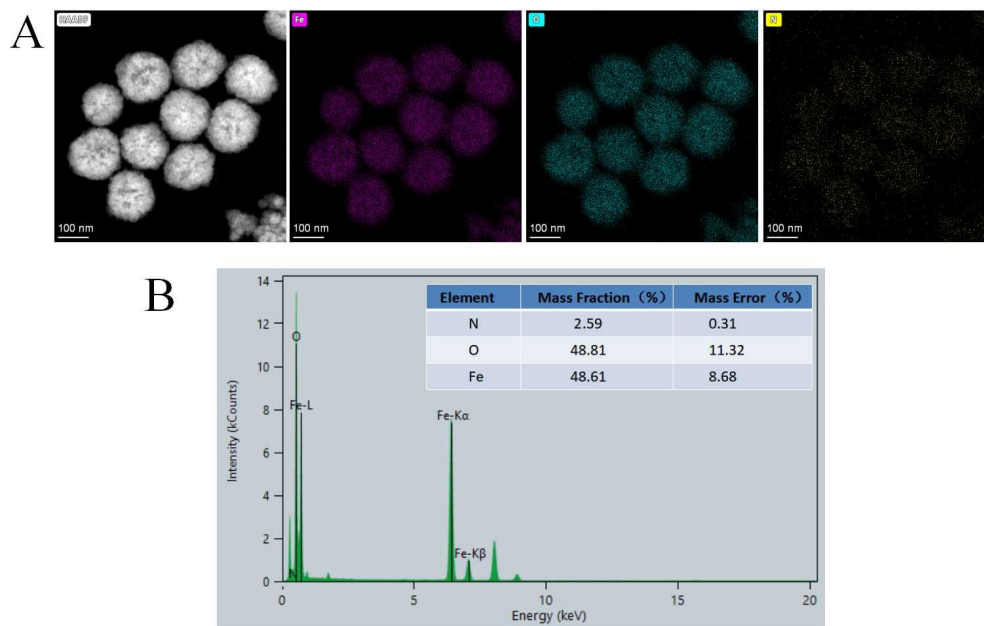


Figure S2. (A) Element mapping images and (B) distribution ration of Fe, O, and N in Fe_3O_4 NPs.

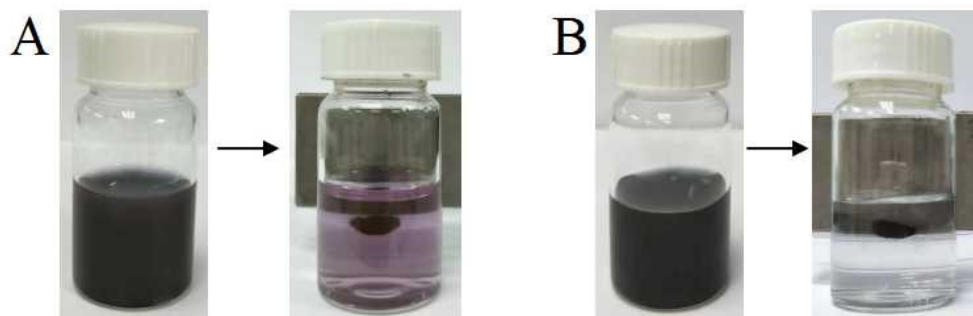


Figure S3. Solution color of $\text{Fe}_3\text{O}_4@Au$ NPs (A) and $\text{Fe}_3\text{O}_4@Au\text{-MBA@PDA}$ NPs (B) after magnetic separation.

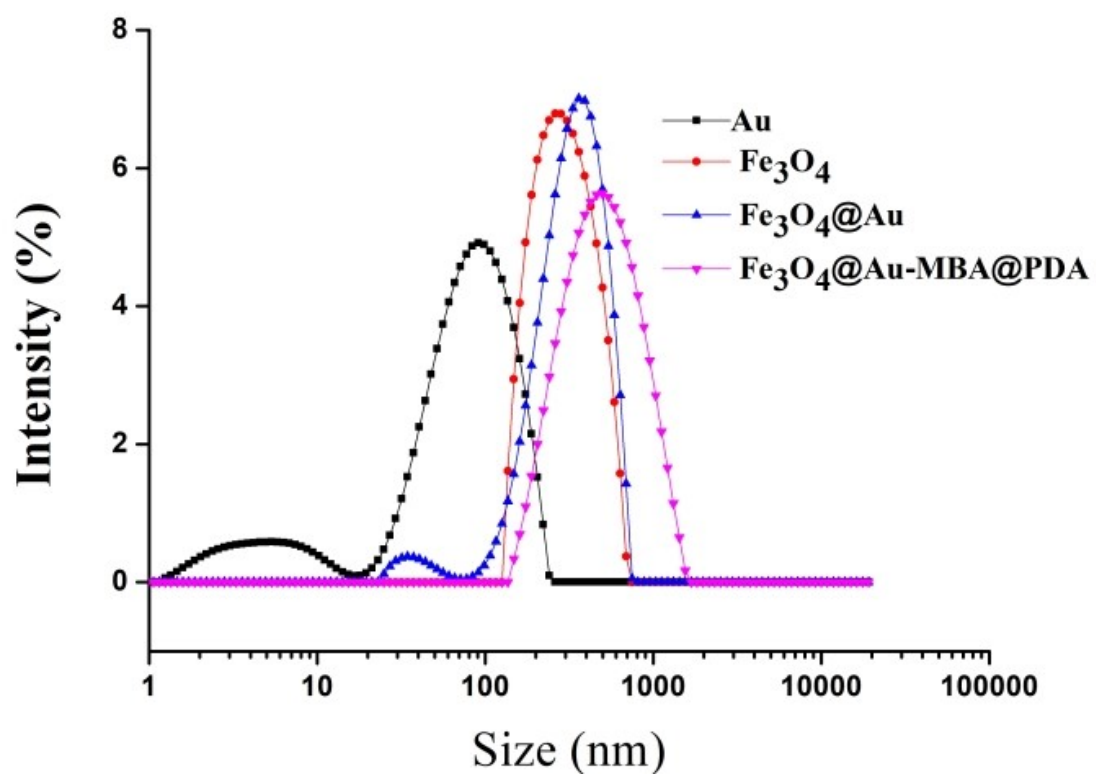


Figure S4. The particle size of Fe₃O₄ NPs (A), Au NPs (B), Fe₃O₄@Au NPs (C) and Fe₃O₄@Au-MBA@PDA (D) measured by DLS, respectively.

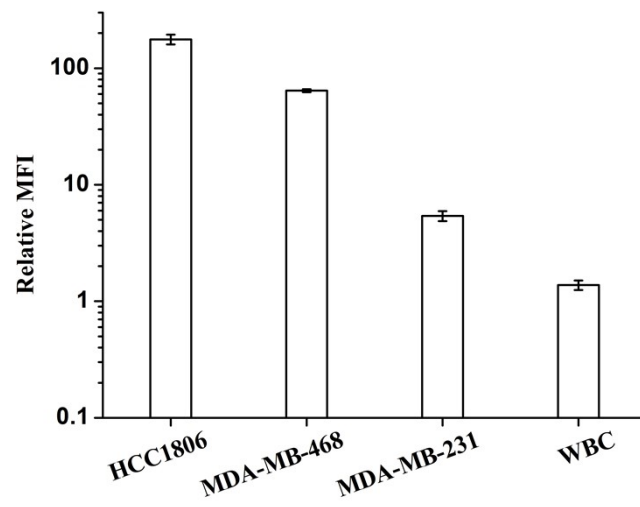


Figure S5. Relative Mean Fluorescence Intensity (MFI) of trop2 protein; MFI of trop2 was normalized using MFI of the IgG in each cell line, respectively.

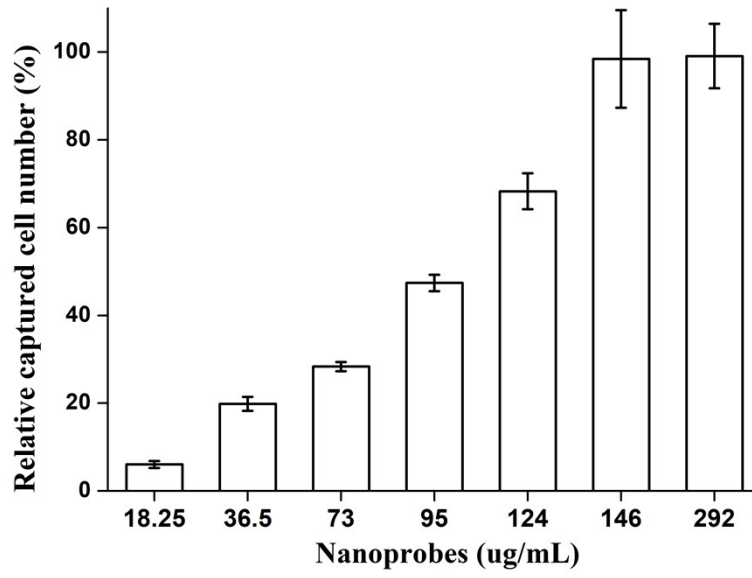


Figure S6 Capture efficiencies of the bioprobes with different concentrations for high trop2-expressing HCC1806 cells.

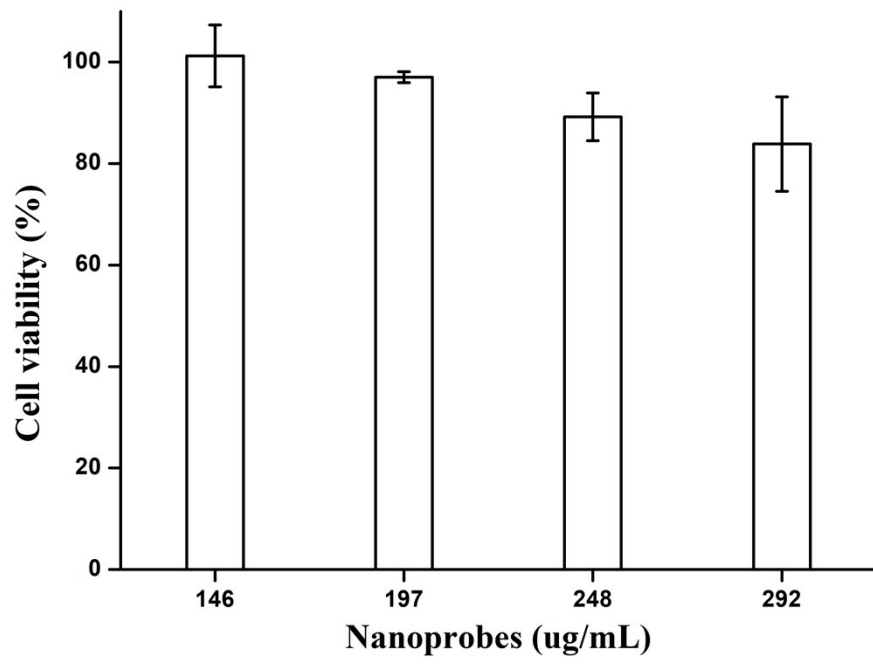


Figure S7. Cytotoxicity of bioprobes at different concentrations on HCC1806 cells within 24 h.

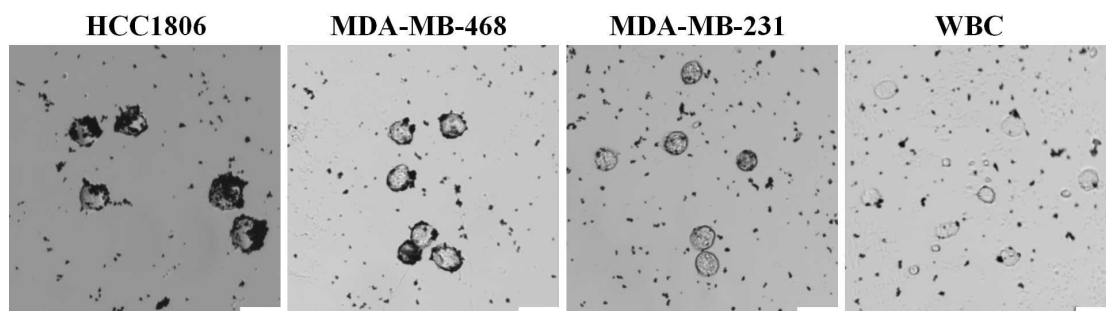


Figure S8. Representative optical microscope images of HCC1806, MDA-MB-468, MDA-MB-231, and WBC incubated with the bioprobes, respectively. Scale bar = 20 μm .

Table S1. Average SERS intensity of TNBC cell lines and WBC. Data were expressed as mean \pm standard deviation.

Group	Average SERS intensity of cells
WBC	147.19 \pm 77.19
MDA-MB-231	242.66 \pm 65.65 ^a
MDA-MB-231	394.97 \pm 125.64 ^{a,b}
HCC1806	848.05 \pm 208.24 ^{a,b,c}

a: p < 0.01 versus WBC group; b: p < 0.01 versus MDA-MB-231 group;

c: p < 0.01 versus MDA-MB-468 group.

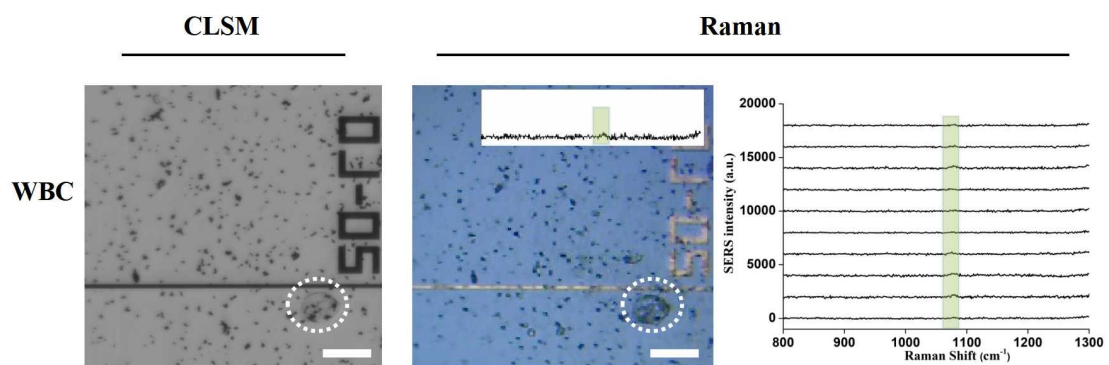


Figure S9. CLSM images and SERS signal of the WBC. Scale bar = 20 μm .

Table S2. SERS detection sensitivity and specificity of the two cut-off values 281 and 206.

cut-off	Number of cells detected				Sensitivity	Specificity
	WBC	MDA-MB-231	MDA-MB-468	HCC1806	(231+468+1806)/30	1-(WBC/10)
281	0	1	8	10	63%	100%
206	2	5	10	10	83%	80%